articles

molecular pharmaceutics

Contrast-Enhanced Magnetic Resonance Angiography with Biodegradable (Gd-DTPA)-Cystamine Copolymers: Comparison with MS-325 in a Swine Model

Thanh D. Nguyen,[§,†] Pascal Spincemaille,[§,†] Anagha Vaidya,[‡] Martin R. Prince,[†] Zheng-Rong Lu,[‡] and Yi Wang*[,§,†]

Department of Radiology, Weill Medical College of Cornell University, New York, New York 10022, Department of Radiology, University of Pittsburgh Medical Center, Pittsburgh, Pennsylvania 15213, and Department of Pharmaceutics and Pharmaceutical Chemistry, University of Utah, Salt Lake City, Utah 84112

Received May 3, 2006

Abstract: The purpose of this study is to evaluate the use of (Gd-DTPA)-cystamine copolymers (GDCC), a novel biodegradable intravascular polydisulfide-based macromolecular gadolinium-(III) contrast agent, for first-pass and steady-state contrast-enhanced magnetic resonance angiography (MRA) in a swine model. A breath-hold background-suppressed 3D MRA of the thorax was performed for first-pass imaging and repeated every 10 min after GDCC injection to monitor the tissue enhancement time course. A navigator-gated 3D MRA of the coronary arteries was performed during steady state following the first-pass imaging. Imaging with intravascular agent MS-325 approximately 1 h after GDCC injection was also included for comparison. Experimental results indicated that GDCC provided significant blood signal-to-noise ratio (SNR) improvement, approximately 1633% for first-pass and 33% for steady-state contrast-enhanced MRA. Compared to MS-325, GDCC provided similar blood enhancement for first-pass and steady-state imaging but with a different tissue enhancement time course. The blood SNR enhancement half-time was 10 ± 6 min for GDCC and 46 ± 33 min for MS-325. GDCC provided less enhancement in the liver, bone growth plates, and muscle than MS-325.

Keywords: Contrast agent; intravascular biodegradable; magnetic resonance angiography; coronary arteries

Introduction

Current clinically available constrast agents for magnetic resonance imaging (MRI) are mostly low molecular weight gadolinium (Gd) chelates which can be used only to perform first-pass contrast-enhanced magnetic resonance angiography (MRA) because of their rapid and massive extravasation in the interstitial space and excretion in the urine.[1] Intravascular contrast agents that have high molecular weight or are capable of binding to serum biomacromolecules can remain in the blood pool for a longer period, allowing contrast-enhanced MRA with a wider range of imaging procedures.[2] The long blood retention of intravascular contrast agents provides a sufficient enhancement window to allow steady-state acquisition of high signal-to-noise ratio (SNR) and high resolution 3D images of the coronary arteries and other vessels.[3−5] Currently, several intravascular contrast agents

* Author to whom correspondence should be addressed. Mailing address: Weill Medical College of Cornell University, Department of Radiology, 575 Lexington Avenue, 3rd Floor, New York, NY 10022. E-mail: yiwang@med.cornell.edu. Phone: (646) 253-2809. Fax: (646) 253-2815.

§ University of Pittsburgh.

† Weill Medical College of Cornell University.

‡ University of Utah.

(1) Prince, M. R.; Grist, T. M.; Debatin, J. F. *3D Contrast MR Angiography*; Springer: Berlin, 2003.

(2) Corot, C.; Violas, X.; Robert, P.; Gagneur, G.; Port M. Comparison of different types of blood pool agents (P792, MS325, USPIO) in a rabbit MR angiography-like protocol. *Invest. Radiol.* **2003**, *38*, 311−319.

10.1021/mp060051o CCC: $33.50
Published on Web 09/02/2006

have been actively investigated in preclinical and clinical development, including MS-325[4,6−8] and B22956[9] which bind with plasma albumin, ultrasmall paramagnetic ion oxide particles,[10,11] dendritic macromolecules,[12−14] and polymeric macromolecules.[15,16] Recently a polydisulfide-based Gd-DTPA cystamine copolymer (GDCC) has been developed as a biodegradable macromolecular contrast agent.[17,18] This agent can be degraded into smaller Gd(III) complexes by cleaving the disulfide bonds in the polymer chains via disulfide−thiol exchange reaction with endogenous thiols. The smaller Gd(III) complexes are rapidly filtered by the kidney. It has been demonstrated that the long-term Gd tissue accumulation of GDCC was comparable to that of Gd-(DTPA-BMA).[19]

The objective of this study was to assess the effectiveness of GDCC in contrast-enhanced MRA in a swine model. A 3D sequence with continuous balanced steady-state free precession (SSFP) acquisition was used to image vessels in the thorax during the first pass after injection.[20] The SSFP sequence was chosen because it provides approximately twice the SNR or twice the Gd detection sensitivity of a standard spoiled gradient echo sequence.[21,22] A real-time navigator-gated ECG-triggered 3D SSFP sequence was then used to image the coronary arteries in steady state.[23] Injection of MS-325, a known intravascular contrast agent, was performed approximately 1 h after GDCC injection for comparison.

Materials and Methods

Experiments were performed using a 1.5 T SIGNA CV/i whole-body MR system (CNV4 software version, GE Healthcare Technologies, Waukesha, WI). A four-element phased-array cardiac coil (two anterior, two posterior elements) was used for signal reception. Animals were positioned supine and feet first.

Animal Preparation. Imaging was performed on seven Yorkshire swines (body weight 34 ± 4 kg). All experimental procedures were in accordance with our Institutional Animal Care and Use Committee guidelines. Each animal was sedated with an intramuscular injection of ketamine (20 mg/kg) and xylazine (2 mg/kg). The animals were then induced

(3) Wang, Y.; Rossman, P. J.; Grimm, R. C.; Wilman, A. H.; Riederer, S. J.; Ehman, R. L. 3D MR angiography of pulmonary arteries using real-time navigator gating and magnetization preparation. *Magn. Reson. Med.* **1996**, *36*, 579−587.

(4) Li, D.; Dolan, R. P.; Walovitch, R. C.; Lauffer, R. B. Three-dimensional MRI of coronary arteries using an intravascular contrast agent. *Magn. Reson. Med.* **1998**, *39*, 1014−1018.

(5) Dirksen, M. S.; Kaandorp, T. A.; Lamb, H. J.; Doornbos, J.; Corot, C.; de Roos, A. Three-dimensional navigator coronary MRA with the aid of a blood pool agent in pigs: improved image quality with inclusion of the contrast agent first-pass. *J. Magn. Reson. Imaging* **2003**, *18*, 502−506.

(6) Lauffer, R. B.; Parmelee, D. J.; Dunham, S. U.; Ouellet, H. S.; Dolan, R. P.; Witte, S.; McMurry, T. J.; Walovitch, R. C. MS-325: albumin-targeted contrast agent for MR angiography. *Radiology* **1998**, *207*, 529−538.

(7) Grist, T. M.; Korosec, F. R.; Peters, D. C.; Witte, S.; Walovitch, R. C.; Dolan, R. P.; Bridson, W. E.; Yucel, E. K.; Mistretta, C. A. Steady-state and dynamic MR angiography with MS-325: initial experience in humans. *Radiology* **1998**, *207*, 539−544.

(8) Stuber, M.; Botnar, R. M.; Danias, P. G.; McConnell, M. V.; Kissinger, K. V.; Yucel, E. K.; Manning, W. J. Contrast agent-enhanced, free-breathing, three-dimensional coronary magnetic resonance angiography. *JMRI* **1999**, *10*, 790−799.

(9) La Noce, A.; Stoelben, S.; Scheffler, K.; Hennig, J.; Lenz, H. M.; La Ferla, R.; Lorusso, V.; Maggioni, F.; Cavagna, F. B22956/1, a new intravascular contrast agent for MRI: first administration to humans-preliminary results. *Acad. Radiol.* **2002**, *9* (Suppl. 2), S404−S406.

(10) Kellar, K. E.; Fujii, D. K.; Gunther, W. H.; Briley-Saebo, K.; Bjornerud, A.; Spiller, M.; Koenig, S. H. NC100150 Injection, a preparation of optimized iron oxide nanoparticles for positive-contrast MR angiography. *J. Magn. Reson. Imaging* **2000**, *11*, 488−494.

(11) Herborn, C. U.; Schmidt, M.; Bruder, O.; Nagel, E.; Shamsi, K.; Barkhausen, J. MR coronary angiography with SH L 643 A: initial experience in patients with coronary artery disease. *Radiology* **2004**, *233*, 567−573.

(12) Misselwitz, B.; Schmitt-Willich, H.; Ebert, W.; Frenzel, T.; Weinmann, H. J. Pharmacokinetics of Gadomer-17, a new dendritic magnetic resonance contrast agent. *Magma* **2001**, *12*, 128−134.

(13) Port, M.; Corot, C.; Raynal, I.; Idee, J. M.; Dencausse, A.; Lancelot, E.; Meyer, D.; Bonnemain, B.; Lautrou, J. Physicochemical and biological evaluation of P792, a rapid-clearance blood-pool agent for magnetic resonance imaging. *Invest. Radiol.* **2001**, *36*, 445−454.

(14) Ruehm, S. G.; Schmitz-Cristina, H.; Violas, X.; Corot, C.; Debatin, J. F. MR angiography with a new rapid clearance blood pool agent (P792): initial experience in rabbits. *Acad. Radiol.* **2002**, *9* (Suppl. 2), S407−S408.

(15) Schuhmann-Giampieri, G.; Schmitt-Willich, H.; Frenzel, T.; Press, W. R.; Weinmann, H. J. In vivo and in vitro evaluation of Gd-DTPA-polylysine as a macromolecular contrast agent for magnetic resonance imaging. *Invest. Radiol.* **1991**, *26*, 969−974.

(16) Weissleder, R.; Bogdanov, A., Jr.; Tung, C. H.; Weinmann, H. J. Size optimization of synthetic graft copolymers for in vivo angiogenesis imaging. *Bioconjugate Chem.* **2001**, *12*, 213−219.

(17) Lu, Z.; Parker, D. L.; Goodrich, K. C.; Wang, X.; Dalle, J.; Buswell, H. R. Extracellular biodegradable macromolecular gadolinium (III) complexes for MRI. *Magn. Reson. Med.* **2004**, *51*, 27−34.

(18) Lu, Z.-R.; Mohs, A. M.; Zong, Y.; Feng, Y. Polydisulfide Gd(III) chelates as biodegradable macromolecular magnetic resonance imaging contrast agents. *Int. J. Nanomed.* **2006**, *1*, 31−40.

(19) Wang, X.; Feng, H. Y.; Ke, T.; Schable, M.; Lu, Z.-R. Pharmacokinetics and long-term Gd tissue accumulation of (Gd-DTPA)-cystamine copolymers, a biodegradable macromolecular MRI contrast agent. *Pharm. Res.* **2005**, *22*, 596−601.

(20) Spincemaille, P.; Nguyen, T. D.; Wang, Y. View ordering for magnetization prepared steady-state free precession acquisition: application in contrast-enhanced MR angiography. *Magn. Reson. Med.* **2004**, *52*, 461−466.

(21) Foo, T. K.; Ho, V. B.; Marcos, H. B.; Hood, M. N.; Choyke, P. L. MR angiography using steady-state free precession. *Magn. Reson. Med.* **2002**, *48*, 699−706.

(22) Scheffler, K.; Lehnhardt, S. Principles and applications of balanced SSFP techniques. *Eur. Radiol.* **2003**, *13*, 2409−2418.

(23) Nguyen, T. D.; Spincemaille, P.; Wang, Y. Improved magnetization preparation for navigator steady-state free precession 3D coronary MR angiography. *Magn. Reson. Med.* **2004**, *51*, 1297−1300.

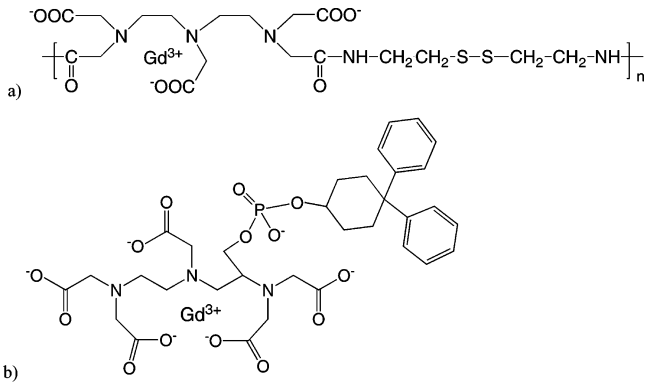

Figure 1. (a) Linear structure of macromolecule GDCC and (b) structure of small molecule MS-325.

Table 1. Physicochemical Characteristics of GDCC and MS-325

characteristics	GDCC	MS-325	
		free	albumin bound
structure	biodegradable macromolecule		
molecular mass (Da)	17 700	957	68 000
T1 relaxivity at 1.5 T (s^{-1} mM^{-1})	4.4	6	25
distribution half-time (min)	1.08 (rat)		0.917 (rat)
elimination half-time (min)	26.5 (rat)		23.1 (rat)

with a sodium thiopental (20 mg/kg body weight) iv, intubated, and maintained on 1.0−3.0% isoflurane and oxygen inhalant anesthesia with mechanical ventilation for the study. In each animal, one jugular vein was cannulated for intravenous infusion of contrast agents. The electrocardiogram (ECG) was monitored throughout the entire duration of the imaging session.

Scout Scans. Prior to constrast injection, sagittal gradient echo scout scans were performed to localize the heart, the aortic root, and the diaphragm. A coronal cine scout scan was acquired to identify the optimal delay time between the ECG trigger and the period of minimal cardiac motion.

Contrast Injection and Imaging Procedure. The chemical structures for GDCC and MS-325 (EPIX Pharmaceuticals, Cambridge, MA) are illustrated in Figure 1, and their physicochemical characteristics are summarized in Table 1 (for a more thorough description of GDCC, see refs 17 and 18). Of the seven pigs, the first animal received GDCC injection only, the second animal received MS-325 injection only, and the remaining five animals received both GDCC and MS-325 injections. GDCC and MS-325 were injected manually at a dose of 0.1 mmol/kg and an injection rate of 1 mL/s, followed by a 20 mL saline flush. In the five pigs that received two injections, the MS-325 injection was performed approximately 60 min after the GDCC injection. First-pass breath-hold 3D MRA of the thorax and steady-state navigator-gated 3D MRA of the coronary arteries were acquired after each injection. In addition, the breath-hold MRA was repeated approximately every 10 min after injection. The imaging procedure is illustrated in Figure 2. Precontrast angiograms were also acquired for comparison.

Breath-Hold Imaging of the Thorax. For first-pass imaging, the sequence was initiated 15 s after the start of contrast infusion, the estimated time required for the contrast bolus to travel from the injection site to the imaging volume. An inversion recovery (IR)-prepared continuous (ungated to ECG) SSFP sequence was used to acquire 3D MRA of the thorax during a 43 s breath-hold (respiratory ventilator off).[20] Inversion pulses were inserted periodically into the rf trains such that data acquisition took place during the nulling of the background signals. A fan view ordering was used to optimize signal contrast and reduce eddy current artifacts.[20] Twenty-six "dummy" rf cycles and 160 data acquisition cycles were played out after each inversion pulse. This inversion frequency was estimated by assuming T1 = 50 ms, T2 = 30 ms for contrast-enhanced blood, T1 = 1000 ms, T2 = 100 ms for background tissue, and an 85% maximal background signal regrowth (see ref 20 for detailed calculation). The coronal imaging volume encompassed the heart, pulmonary vessels, and the descending aorta. Other scanning parameters were TR = 4.2 ms, TE = 1.4 ms (asymmetric partial echo), flip angle = 60°, receiver bandwidth = ±62.5 kHz, FOV = 26 cm, slice thickness = 2.4 mm, 48 slices, in-plane resolution = 1.0 × 1.6 mm^2.

Navigator-Gated Imaging of the Coronary Arteries. Immediately following the first-pass breath-hold imaging of the thorax, steady-state navigator-gated 3D coronary MRA was obtained using an ECG-triggered segmented *k*-space SSFP sequence. An optimized magnetization preparation scheme that improves intrinsic SSFP contrast and minimizes the delay between the navigator echo and the image echoes was used.[23] Due to pulse sequence and real-time navigating system preparations, actual data acquisition started 3−3.5 min after the start of contrast infusion. The scanning parameters were TR = 4.2 ms, TE = 1.4 ms (asymmetric partial echo), flip angle = 60°, receiver bandwidth = ±62.5 kHz, slice thickness = 3 mm, 18 slices, FOV = 260 mm, in-plane resolution = 1.0 × 1.0 mm^2, sequential view ordering along k_z, 18 echoes per heartbeat (corresponding to an acquisition window of 76 ms). Data were acquired from an axial slab covering the right coronary artery (RCA) and the left main coronary artery (LM). The acquisition time was 256 heartbeats assuming 100% navigator acceptance rate.

A pencil-beam navigator was acquired from a superior−inferior cylinder of tissue through the dome of the right hemidiaphragm, and displacements were extracted using a least-squares algorithm.[24] The phase-ordered automatic window selection (PAWS) gating algorithm, which optimizes gating window selection and minimizes residual motion artifacts within the gating window,[25] was implemented on a Sun workstation (Ultra1; Sun Microsystems, Palo Alto, CA) to control data acquisition in real time. A gating window of 3 mm was used. Real-time access to the scanner's raw data

(24) Wang, Y.; Grimm, R. C.; Felmlee, J. P.; Riederer, S. J.; Ehman, R. L. Algorithms for extracting motion information from navigator echoes. *Magn. Reson. Med.* **1996**, *36*, 117−123.

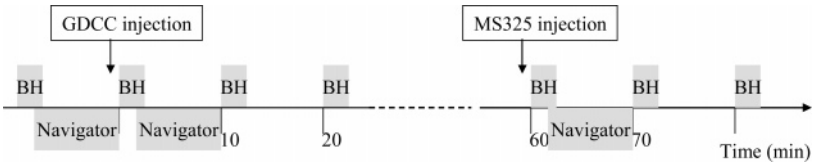

Figure 2. Flowchart for contrast injection and imaging in the swine experiment. (Timing is approximate.)

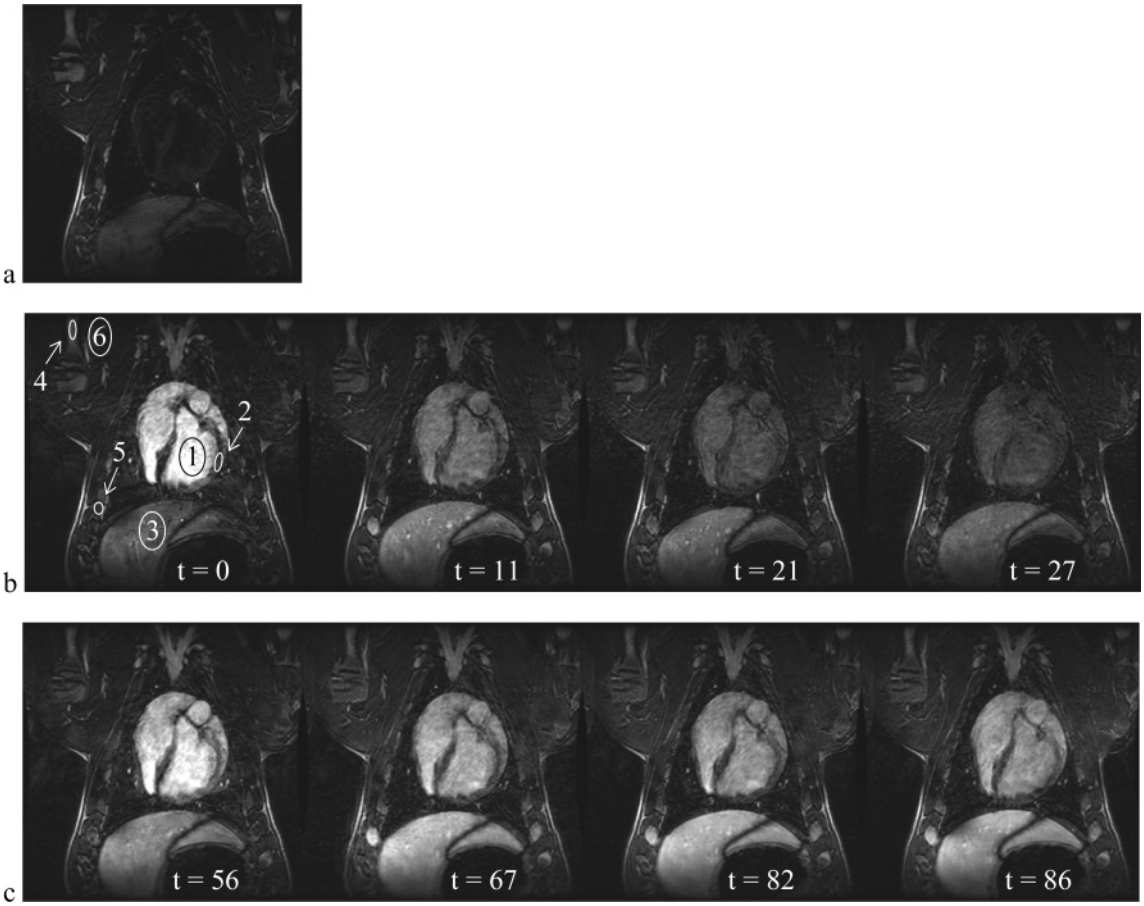

Figure 3. Tissue enhancement as a function of time (in minutes) obtained in pig C (a) precontrast, (b) after the first injection of GDCC at $t = 0$, and (c) after a second injection of MS-325 at $t = 56$ min. The $t = 0$ image shows the six different regions of interest from which signal was measured: (1) blood, (2) myocardium, (3) liver, (4) leg bone, (5) rib, and (6) leg muscle.

and instruction memory from the workstation was made possible through a high-speed adapter (SBS Bit 3 Operations, St. Paul, MN).

Image Analysis. For image quality comparison between precontrast, post-GDCC, and post-MS-325 acquisitions in breath-hold first-pass MRA, blood, myocardium, liver, rib, muscle, and bone signals were measured in regions of interest (ROI) positioned within the left ventricular (LV) blood pool, LV wall, the region of liver immediately below the heart, the right-inferior rib, and the muscle and bone of the right upper leg, respectively (Figure 3). Contrast enhancement time courses were then obtained from the serial breath-hold imaging for both contrast agents. The blood SNR time course after each injection was fitted to an exponentially decaying function at the experimentally sampled time points, and the blood SNR half-time was measured to be the time at which the SNR had decreased by 50%. For navigator-gated coronary MRA, blood and myocardium signals were measured in ROIs positioned in adjacent areas of the LV blood pool and the myocardium, respectively (Figure 4). All measurements were obtained from a middle slice of the source 3D data set using similar anatomical locations in all animals. Noise standard deviation (σ_n) was estimated from the background air. SNR and contrast-to-noise ratio (CNR) were defined as follows: $\mathrm{SNR} = S/\sigma_n$, $\mathrm{CNR} = (S - S_0)/\sigma_n$,

(25) Jhooti, P.; Gatehouse, P. D.; Keegan, J.; Bunce, N. H.; Taylor, A. M.; Firmin, D. N. Phase ordering with automatic window selection (PAWS): a novel motion-resistant technique for 3D coronary imaging. *Magn. Reson. Med.* **2000**, *43*, 470−480.

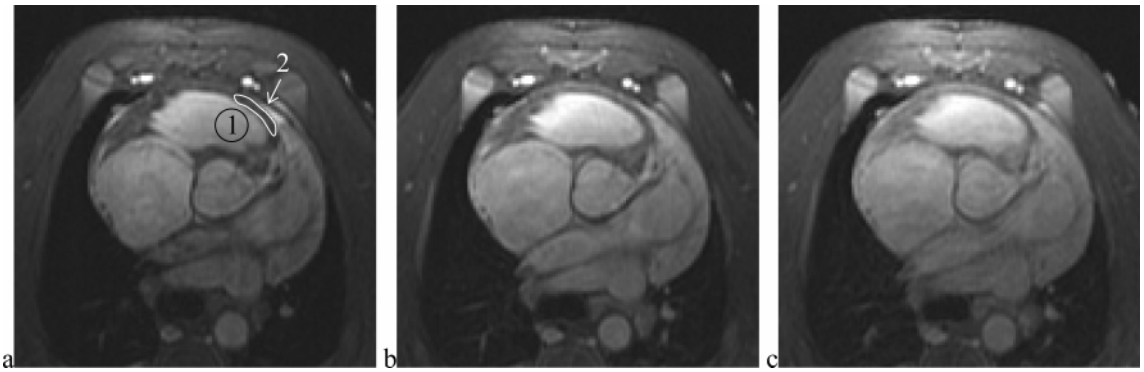

Figure 4. Steady-state navigator-gated 3D MRA of the coronary arteries. Source images of the left main coronary artery acquired (a) precontrast, (b) post-GDCC, and (c) post-MS-325 in pig C. Improved vessel delineation is depicted in panel b. The typical regions of interest from which (1) blood and (2) myocardium signals were measured are shown in panel a.

Table 2. Postcontrast SNR and CNR of First-Pass Breath-Hold 3D MRA for GDCC and MS-325[a]

	blood SNR			blood-to-muscle CNR		
pig	precontrast	post-GDCC	post-MS-325	precontrast	post-GDCC	post-MS-325
A	8	157	X	−3	146	X
B	7	X	85	1	X	79
C	4	136	101	−1	130	96
D	6	118	102	2	113	96
E	25	134	147	17	124	133
F	6	143	147	−1	135	139
G	6	163	135	4	160	131
mean ± SD	9 ± 7	142 ± 16	119 ± 27	3 ± 7	135 ± 16	112 ± 25
p						
post- vs precontrast		0.000 01	0.0001		0.000 02	0.000 08
GDCC vs MS-325			0.25			0.2

[a] Precontrast values are included for comparison (X = unavailable data).

where S and S_0 denote the tissue signals of interest. Two-tailed paired sample t tests were performed to determine the statistical significance of SNR and CNR differences between the precontrast, post-GDCC, and post-MS-325 images.

Results

First-pass breath-hold 3D thoracic MRA experiments were completed successfully on all seven pigs. For steady-state navigator-gated 3D coronary MRA, one pig died unexpectedly and another pig woke up from anesthesia during scanning after the MS-325 injection, causing the acquired image data to be excluded from further analysis. The average scan times for the navigator-gated GDCC and MS-325 acquisitions were 371 ± 85 and 352 ± 66 s, respectively. The measured SNR and CNR are summarized in Tables 2 and 3.

For first-pass breath-hold 3D thoracic MRA, excellent background suppression was obtained in both precontrast (n = 7) and postcontrast (n = 6) images with the periodic IR preparation. Both GDCC and MS-325 provided significant improvement in blood signal (Table 2). Compared to MS-325 (n = 5), GDCC provides slightly but insignificantly higher blood SNR (p = 0.25) and blood-to-muscle CNR (p = 0.2).

For steady-state navigator-gated 3D coronary MRA, the average blood SNR of the post-GDCC (n = 6) and post-MS-325 (n = 4) images were improved over the precontrast images by 33% (p = 0.004) and 16% (p = 0.015), respectively (Table 3). However, there was no significant improvement (p = 0.58) and a decrease of 23% (p = 0.14) in the blood-to-myocardium CNR of the post-GDCC and post-MS-325 images, respectively. Compared to MS-325 (n = 3), GDCC provided slightly better but insignificant vascular enhancement (p = 0.18) and less myocardial enhancement (p = 0.01).

Figure 3 shows example breath-hold images acquired at different time points before and after contrast injection. Figure 4 illustrates a case in which GDCC provided better coronary artery delineation for steady-state imaging. Figure 5 demonstrates that both GDCC and MS-325 markedly improved the visualization of the thoracic vessel branches and the heart for first-pass breath-hold imaging.

Figure 6 shows the signal enhancement curves as a function of time for six tissues—blood, myocardium, liver, leg bone, rib, and leg muscle—obtained from the same pig. In this animal, the blood SNR half-times for GDCC and MS-325 were 10 and 45 min, respectively. The postcontrast blood SNR time curves were well approximated by an exponentially decaying function with a goodness of fit of 0.99 and

Table 3. Postcontrast SNR and CNR of Steady-State Navigator-Gated 3D Coronary MRA for GDCC and MS-325[a]

	blood SNR			blood-to-myocardium CNR		
pig	precontrast	post-GDCC	post-MS-325	precontrast	post-GDCC	post-MS-325
A	89	126	X	41	52	X
B	67	X	88	40	X	44
C	115	160	137	68	80	59
D	98	131	110	60	69	38
E	117	137	X	64	68	X
F	127	136	136	63	60	36
G	102	123	X	68	50	X
mean ± SD	102 ± 20	135 ± 13	118 ± 23	58 ± 12	63 ± 11	44 ± 10
p						
post- vs precontrast		0.004	0.015		0.58	0.14
GDCC vs MS-325			0.18			0.01

[a] Precontrast values are included for comparison (X = unavailable data).

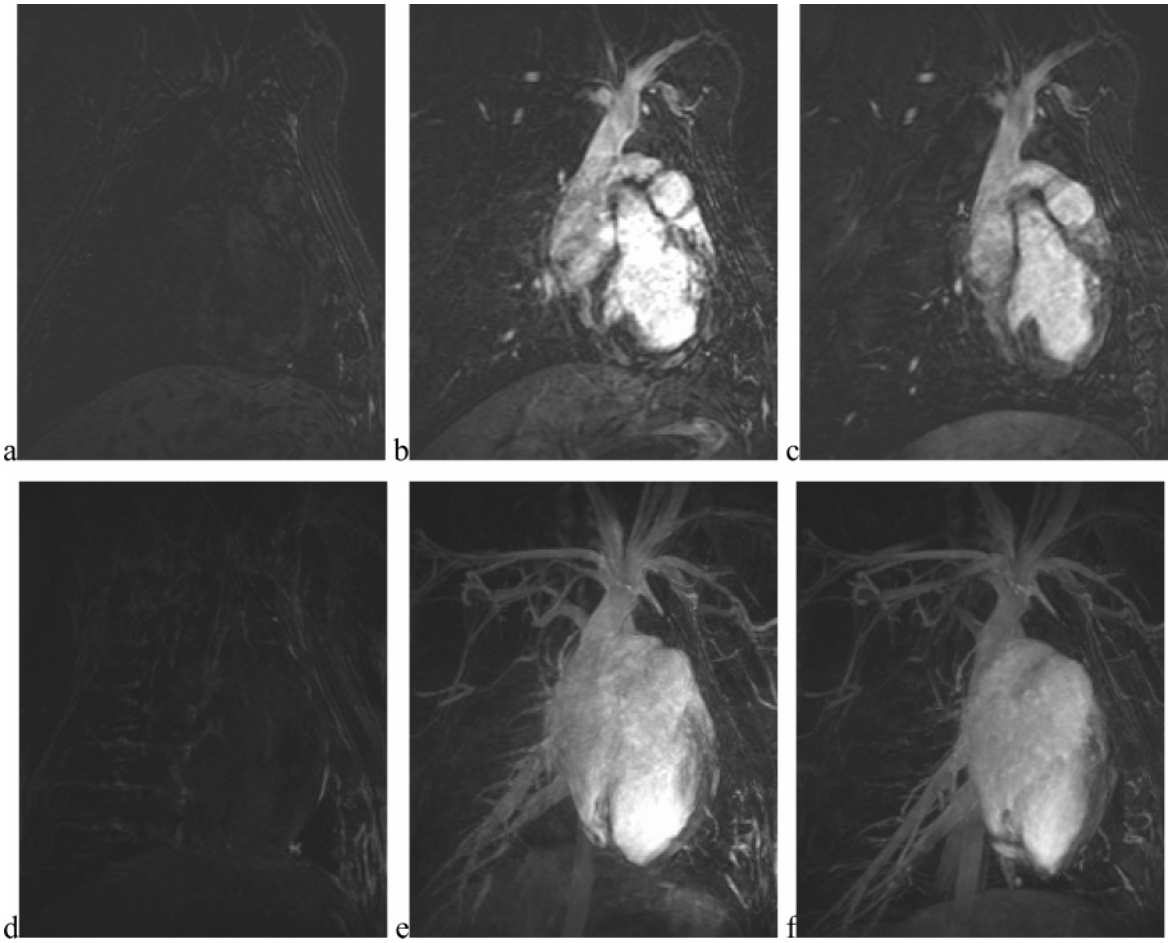

Figure 5. First-pass breath-hold 3D MRA of the thorax. Source images acquired (a) precontrast, (b) post-GDCC, and (c) post-MS-325 in pig C. Corresponding MIP images acquired (d) precontrast, (e) post-GDCC, and (f) post-MS-325. Excellent background suppression is depicted in all images. GDCC and MS-325 images show drastically improved blood SNR compared to precontrast images.

0.97 for GDCC and MS-325, respectively (Figure 6a). Over all animals ($n = 6$), the average blood SNR half-time was 10 ± 6 min for GDCC and 46 ± 33 min for MS-325. MS-325 had a longer presence in the blood than GDCC ($p = 0.04$), leading to a longer window of blood enhancement (Figures 3 and 6a). The average myocardial signal increased by 290 ± 103% for GDCC and 471 ± 96% for MS-325 during the first pass and decayed after that (with a 23 ± 10 min half-time for GDCC). The average liver signal during first-pass was found to be 145 ± 68% and 201 ± 87% higher than the precontrast value for GDCC and MS-325, respectively. The liver signal evolution profile for MS-325 typically

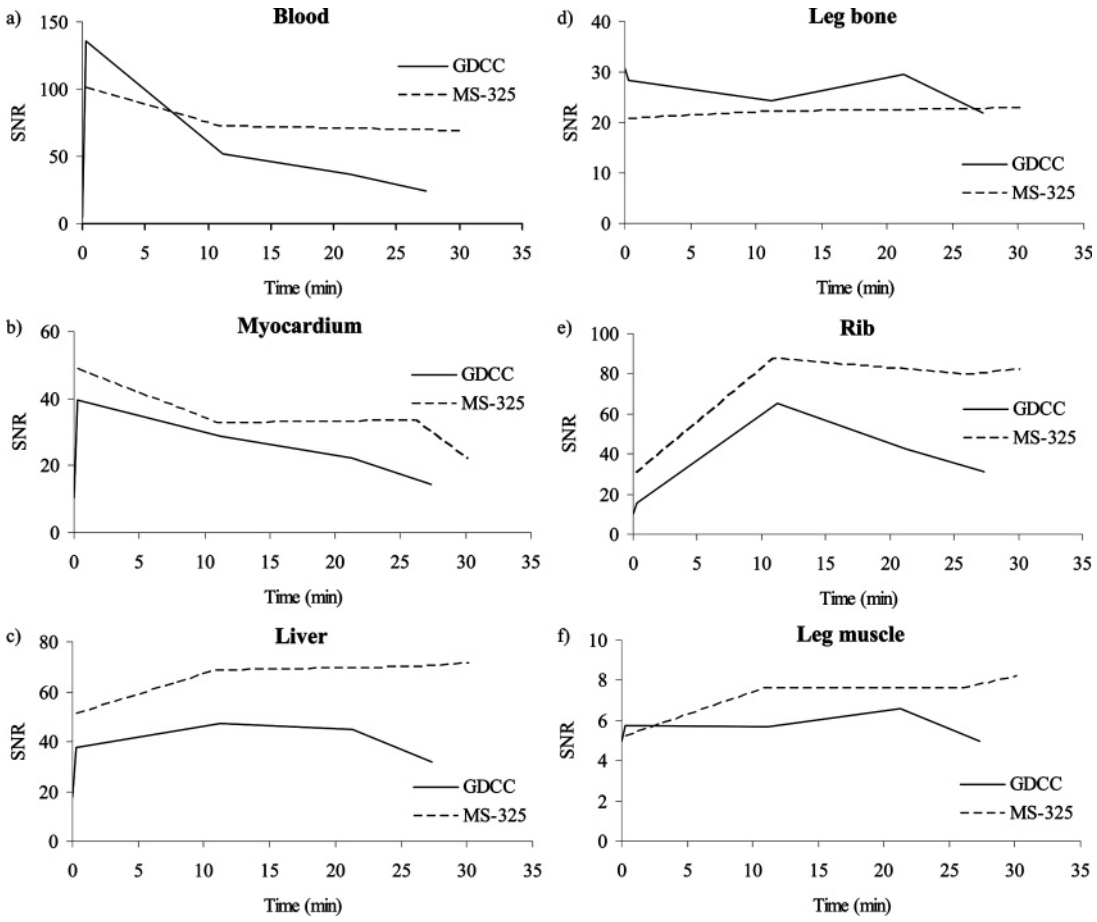

Figure 6. SNR time course for (a) blood, (b) myocardium, (c) liver, (d) leg bone, (e) rib, and (f) leg muscle in pig C after the injection of GDCC and MS-325, respectively. Times are shown relative to the injection time of each contrast agent. Precontrast values are included for comparison.

demonstrated a long signal plateau after an initial increase (Figure 6c). The leg bone signal was only slightly affected by the injection of contrast agents (Figure 6d). An initial steep increase in the rib signal was typically observed for both contrast agents. Following this period, the rib signal stayed fairly constant or kept increasing slightly over time for MS-325, while it peaked around 10 min after the injection of GDCC (Figure 6e). The average leg muscle signal was found to increase 12 ± 7% and 21 ± 23% over precontrast level for GDCC and MS-325, respectively.

Discussion

The polydisulfide-based (Gd-DTPA)-cystamine copolymer (GDCC) is a biodegradable intravascular macromolecular MRI contrast agent with rapid renal clearance. The preliminary in vivo data reported here have shown that this biodegradable intravascular agent provides approximately 10 min of blood enhancement in a pig model, allowing effective first-pass and steady-state imaging for contrast-enhanced MRA. GDCC offers similar blood enhancement to MS-325 for first-pass and steady-state MRA in the first 5−10 min postinjection, and has a shorter blood enhancement duration than that of MS-325 (46 min). Our data also demonstrate that GDCC has different enhancement time courses than MS-325 in liver, rib, and leg muscle.

The observed blood enhancement time courses for GDCC and MS-325 in this pig experiment are different from those observed in a rat model (see similar distribution half-time and elimination half-time in Table 1).[17] A possible explanation is that the binding of MS-325 to rat plasma albumin is different from that to pig plasma albumin. The 10 min blood SNR half-time of GDCC is a reasonable balance between being long enough for navigator-gated 3D coronary MRA and being short enough to allow multiple injections within the same day or the same imaging session. The 46 min blood SNR half-time of MS-325 has the advantage of a long imaging period but is too long to allow repeated injection in the same examination. The blood SNR in breath-hold imaging 30 min after the injection of GDCC returns to almost preinjection level (Figure 6a), indicating effective and rapid renal clearance after GDCC biodegradation. MS-325 resulted in greater liver enhancement, which may reflect the high albumin content of the liver where albumin is produced. Because the binding of MS-325 to plasma albumin is not 100% and is reversible, and because free MS-325 can easily extravasate into interstitial spaces, there is a greater retention of MS-325 in tissue such as liver, rib, and leg muscle than there is of GDCC (Figure 6). These characteristics of the tissue enhancement time courses of GDCC and MS-325 may

be explored for assessing tissue function, such as identifying myocardial scar tissue.

The use of the periodic IR preparation pulse in the breath-hold imaging allowed effective suppression of background tissue and high signal sensitivity to contrast enhancement, but also caused a large standard deviation in the estimation of enhancement ratio between post- and precontrast enhancement signals. For steady-state imaging of navigator-gated coronary MRA, significant improvements in coronary blood SNR after GDCC and MS-325 injections were observed. However, the blood-to-myocardium CNR was improved marginally with GDCC and decreased with MS-325. Because coronary MRA data were acquired only in a brief period in mid-diastole, the substantial magnetization recovery in each cardiac cycle made signal less sensitive to contrast enhancement. The use of IR preparation in each cardiac cycle in contrast-enhanced coronary MRA[26] may improve the blood-to-myocardium CNR. The IR preparation pulse cannot be used in nonenhanced coronary MRA, and accordingly it was not employed in this study to avoid the use of two different pulse sequences for pre- and postcontrast imaging.

It is interesting to note that similar blood enhancement was observed for GDCC and MS-325 in both first-pass thoracic SSFP and steady-state coronary SSFP imaging, although the T1 and T2 relaxivities in blood of GDCC (4.4 and 5.6 mM^{-1} s^{-1} at 1.5 T),[17] on the same order as Gd-DTPA (4.3 and 4.4 mM^{-1} s^{-1}),[27] are substantially smaller than those of MS-325 (19 and 37 mM^{-1} s^{-1}).[27] Unlike T1-weighted spoiled gradient echo (SPGR) imaging where blood enhancement increases with contrast agent relaxivity, SSFP imaging is weighted by T2/T1, which may not be sensitive to agent relaxivity.[28] In our experiment (approximate pig body weight of 35 kg and blood pool volume of 1.5 L), the unenhanced T1/T2 ratio of blood at 1.5 T is 1200 ms/130 ms or 9.2, and the enhanced T1/T2 ratios are 158 ms/68 ms or 2.3 for GDCC and 41 ms/19 ms or 2.2 for MS-325. Accordingly, the enhanced blood signals for GDCC and MS-325 are very similar, $0.33M_0$ and $0.34\ M_0$, respectively (M_0 is the equilibrium magnetization). This explains the observed similar blood enhancement by GDCC and MS-325. In general, SSFP signal enhancement is very sensitive to a small amount of contrast agent and the enhancement rapidly becomes saturated as the contrast dose increases, unlike SGPR imaging where the enhancement effect is approximately linear over a large range of contrast dose.[21]

A major challenge in this study was to maintain the desirable animal condition for the long experiment. This was complicated in part by the quality of the supplied pigs, one of which had lymphoma identified on MRI. Because GDCC has shorter half-time in tissue than MS-325 and assessing the effectiveness of first-pass and steady-state imaging using GDCC was the primary goal of this study, MS-325 was administered after GDCC in all pigs. The time delay between the injections of GDCC and MS-325 was kept relatively short (approximately 1 h). While the blood signal has returned to baseline prior to the MS-325 injection, tissues in other organs may have residual GDCC enhancement, which has limited our quantitative data fitting to blood signal. Additionally, due to the long delay (about 2 h) between the start of animal preparation and the injection of the second contrast dosage, we were unable to obtain MS-325-enhanced data on two pigs, which may degrade the statistical comparison between MS-325 and GDCC for navigator-gated coronary MRA. An experimental design for rigorous comparison between GDCC and MS-325 may consist of imaging pigs on two separate days and randomizing the injection orders between GDCC and MS-325.

In summary, we have successfully demonstrated the feasibility of the experimental intravascular biodegradable (Gd-DTPA)-cystamine copolymer contrast agent for first-pass and steady-state 3D MRA in a swine model.

Acknowledgment. The authors are grateful to David Fisher and Amanda Robinson for their assistance in animal preparation, and to Bryan Kressler for his help with linguistic issues.

MP060051O

(26) Deshpande, V. S.; Li, D. Contrast-enhanced coronary artery imaging using 3D trueFISP. *Magn. Reson. Med.* **2003**, *50*, 570−577.

(27) Rohrer, M.; Bauer, H.; Mintorovitch, J.; Requardt, M.; Weinmann, H. Comparison of magnetic properties of MRI contrast media solutions at different magnetic field strengths. *Invest. Radiol.* **2005**, *40*, 715−724.

(28) Haacke, E. M.; Brown, R. W.; Thompson, M. R.; Venkatesan, R. *Magnetic resonance imaging—physical principles and sequence design*. Wiley-Liss: New York, 1999.